ACS Partner Journal

Journal of the American Society for Mass Spectrometry

pubs.acs.org/jasms

Research Article

Capillary Zone Electrophoresis-Electron-Capture Collision-Induced Dissociation on a Quadrupole Time-of-Flight Mass Spectrometer for Top-Down Characterization of Intact Proteins

Xiaojing Shen,[#] Tian Xu,[#] Blake Hakkila, Mike Hare, Qianjie Wang, Qianyi Wang, Joseph S. Beckman, and Liangliang Sun*

Cite This: https://doi.org/10.1021/jasms.0c00484

Read Online

ACCESS | Metrics & More | Article Recommendations | Supporting Information

ABSTRACT: Mass spectrometry (MS)-based denaturing top-down proteomics (dTDP) requires high-capacity separation and extensive gas-phase fragmentation of proteoforms. Herein, we coupled capillary zone electrophoresis (CZE) to electron-capture collision-induced dissociation (ECciD) on an Agilent 6545 XT quadrupole time-of-flight (Q-TOF) mass spectrometer for dTDP for the first time. During ECciD, the protein ions were first fragmented using ECD, followed by further activation and fragmentation by applying a CID potential. In this pilot study, we optimized the CZE-ECciD method for small proteins (lower than 20 kDa) regarding the charge state of protein parent ions for fragmentation and the CID potential applied to maximize the protein backbone cleavage coverage and the number of sequence-informative fragment ions. The CZE-ECciD Q-TOF platform provided extensive backbone cleavage coverage for three standard proteins lower than 20 kDa from only single charge states in a single CZE-MS/MS run in the targeted MS/MS mode, including ubiquitin (97%, +7, 8.6 kDa), superoxide dismutase (SOD, 87%, +17, 16 kDa), and myoglobin (90%, +16, 17 kDa). The CZE-ECciD method produced comparable cleavage coverage of small proteins (i.e., myoglobin) with direct-infusion MS studies using electron transfer dissociation (ETD), activated ion-ETD, and combinations of ETD and collision-based fragmentation on high-end orbitrap mass spectrometers. The results render CZE-ECciD a new tool for dTDP to enhance both separation and gas-phase fragmentation of proteoforms.

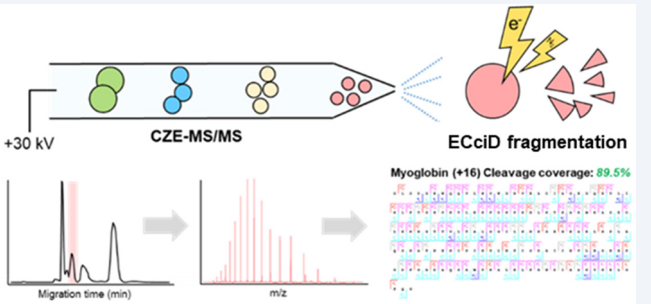

KEYWORDS: *capillary zone electrophoresis-mass spectrometry, electron capture dissociation, collision-induced dissociation, top-down proteomics, quadrupole time-of-flight mass spectrometer, proteoform*

INTRODUCTION

Proteoforms represent all kinds of forms of protein molecules derived from the same gene due to genetic variations, alternative RNA splicing, and post-translational modifications (PTMs).[1] Delineation of proteoforms in cells plays a central role in accurate understanding of protein function in biological processes because different proteoforms from the same gene can have divergent functions.[1−6] Mass spectrometry (MS) based denaturing top-down proteomics (dTDP) aims to comprehensively characterize proteoforms in cells, which needs high-capacity liquid-phase separation and extensive gas-phase fragmentation of proteoforms.[7,8]

Liquid chromatography-MS (LC-MS), typically reversed-phase LC (RPLC), is routinely used for dTDP.[9−17] The proteomes have extremely high complexity if we consider the number of possible proteoforms in them. For example, over one million proteoforms have been predicted in the human proteome.[18] The high sample complexity leads to a high need for liquid-phase separation methods with much better separation capacity for proteoforms. Capillary zone electrophoresis (CZE)-MS has been investigated by our group and others for high-capacity separation of proteoforms, enabling large-scale delineation of proteoforms in complex biological systems.[19−27] CZE-MS has been proven as an alternative tool to RPLC-MS for dTDP due to several valuable features, such as better sensitivity than RPLC-MS,[28,29] high separation efficiency for proteoforms,[21] and great potential for accurate prediction of proteoforms' electrophoretic mobility.[30−32] The tremendous progress of developing robust and highly sensitive CE-MS interfaces has laid a solid foundation for deploying CZE-MS for dTDP.[33−37]

Special Issue: Focus: Top-Down Proteomics: Technology Advances and Biomedical Applications

Received: December 31, 2020
Revised: March 8, 2021
Accepted: March 8, 2021

The need for more comprehensive gas-phase fragmentation of proteoforms requires new fragmentation methods. Collision-based methods, i.e., collision-induced dissociation (CID) and higher-energy collisional dissociation (HCD), are the routine approaches for fragmentation of biomolecules.[11−13,19−22] However, CID and HCD have some bias in backbone cleavages, impeding complete cleavages of proteoforms' backbones. Alternative gas-phase fragmentation techniques have been developed to provide better characterization of large biomolecules, including but not limited to electron-transfer dissociation (ETD),[10,38−40] electron-capture dissociation (ECD),[41−45] and ultraviolet photodissociation (UVPD).[46−49]

ECD for protein fragmentation was pioneered by the McLafferty group in the late 1990s.[50,51] ECD-based protein fragmentation is a nonergodic process, in which electrons are captured at the protonated sites of positively charged protein ions and energetic hydrogen atoms ($H^{\bullet}$) are ejected from the protein ions and are captured at high-affinity sites of the protein ions such as backbone amide, leading to backbone cleavages with the production of c and $z^{\bullet}$ ions.[51] ECD fragmentation can be improved by activating the ECD fragment ions, e.g., collision with gas molecules, to break their intramolecular noncovalent bonds, a process called activated-ion ECD (AI-ECD).[52,53] Ge et al. obtained an efficient characterization of large intact proteins (45 kDa) using the AI-ECD method in 2002 on a Fourier transform (FT) ion cyclotron resonance (ICR) mass spectrometer.[53] The FT-ICR mass spectrometer equipped with ECD has also been employed for the characterization of integral membrane proteins and large protein complexes.[41,54] More recently, an ECD cell has been integrated into QqQ,[42] Q-TOF,[43] ion mobility,[55] and orbitrap[44,56,57] mass spectrometers for peptide, protein, and protein complex fragmentation. Fort et al. demonstrated that ECD outperformed HCD for fragmentation of ubiquitin and myoglobin on an orbitrap mass spectrometer regarding the backbone cleavage coverage.[56] Shaw et al. reported a 93% backbone cleavage coverage for carbonic anhydrase II (29 kDa) using ECD on an orbitrap mass spectrometer with a direct-infusion approach,[44] demonstrating the great potential of ECD to advance dTDP via offering extensive protein fragmentation. Direct-infusion MS is typically deployed for ECD-based TDP, and in-front liquid-phase separation is needed to analyze complex protein mixtures.

In this work, for the first time, we coupled CZE to ECD on a Q-TOF mass spectrometer for highly efficient liquid-phase separation and extensive gas-phase fragmentation of small intact proteins (lower than 20 kDa). An electron-capture collision-induced dissociation (ECciD) was evaluated that employed ECD and CID successively for protein fragmentation. We used the online CZE-ECciD Q-TOF platform to characterize a standard protein mixture in the targeted MS/MS mode. We optimized the charge states of protein precursor ions and the CID potential to maximize the backbone cleavage coverage of proteins from ECciD.

EXPERIMENTAL PROCEDURES

Materials and Chemicals. All standard proteins, ammonium acetate (NH_4Ac), dithiothreitol (DTT), iodoacetamide (IAA), and Microcon-30 kDa centrifugal filter units for buffer exchange were purchased from Sigma-Aldrich (St. Louis, MO). LC/MS grade water, methanol, formic acid (FA), and acetic acid (AA) were purchased from Fisher Scientific (Pittsburgh, PA). Urea was purchased from Alfa Aesar (Tewksbury, MA). Hydrofluoric acid (HF) and acrylamide were purchased from Acros Organics (Fair Lawn, NJ). The fused silica capillary (50 μm i.d., 360 μm o.d.) was purchased from Polymicro Technologies (Phoenix, AZ).

Sample Preparation. A mixture of standard proteins consisting of ubiquitin (bovine, 8.6 kDa, 0.05 mg/mL), myoglobin (equine, 17 kDa, 0.1 mg/mL), carbonic anhydrase (CA, bovine, 29 kDa, 0.5 mg/mL), and bovine serum albumin (BSA, 66 kDa, 2.0 mg/mL) was prepared in 50 mM NH_4HCO_3(pH 8.0) for the charge-state study using targeted MS/MS. For the CID potential study using targeted MS/MS, a standard protein mixture containing ubiquitin (0.05 mg/mL), myoglobin (0.2 mg/mL), and CA (1 mg/mL) was used. Carbonic anhydrase and its impurity superoxide dismutase (SOD, bovine, 16 kDa)[21] were denatured with 8 M urea at 37 °C, reduced with DTT, and alkylated with IAA, followed by buffer exchange with a Microcon-30 kDa centrifugal filter unit. For the buffer exchange, 200 μg protein material was loaded on the membrane and centrifuged at 14000g to remove the sample buffer. Then the sample was washed with 200 μL 50 mM NH_4HCO_3(pH 8.0) for three times, followed by protein recovery from the membrane using 30 μL 50 mM NH_4HCO_3 (pH 8.0) with pipetting and gentle vortexing.

CZE-ESI-MS/MS Analysis. An EMASS-II CE-MS Ion Source commercialized by CMP Scientific (Brooklyn, NY) was used to couple CZE to a 6545XT AdvanceBio Q-TOF (Agilent Technologies) mass spectrometer, Figure 1A.[34,35] The ECD fragmentation was achieved by a built-in electromagnetostatic ExD cell (e-MSion, Corvallis, OR) between the quadrupole and the CID cell, Figure 1B.

A 7100 CE System from Agilent Technologies (Santa Clara, CA) was used for automated operation of CZE. A 75 cm long capillary (50 μm i.d., 360 μm o.d.) coated with linear polyacrylamide (LPA) with one end etched with hydrofluoric acid was used for separation.[58−60] The background electrolyte (BGE) for CZE was 5% (v/v) AA (pH ∼ 2.4). The sheath buffer was 0.2% (v/v) FA containing 10% (v/v) methanol. High voltage (+30 kV) was applied for CZE separation. For each CZE-MS/MS run, 120 nL of the sample was injected into the capillary by applying 100 mbar air pressure for 56 s based on Poiseuille's law. The ESI emitters of the CE-MS interface were pulled from borosilicate glass capillaries (1.0 mm o.d., 0.75 mm i.d., 10 cm length) with a Sutter P-1000 flaming/brown micropipette puller. The opening size of the ESI emitters was 20−30 μm. The voltage for ESI ranged from +2.0 to +2.3 kV.

A 6545XT AdvanceBio Q-TOF (Agilent) was used for the experiments. The gas temperature and flow rate of nitrogen drying gas was 325 °C and 1 L/min. The voltage applied on the ion transfer capillary was 0 V. The fragmentor was 175 V and the skimmer was 65 V. The mass range was set to Standard (3200 m/z). The slicer mode was High Resolution. The instrument mode was Extended Dynamic Range (2 GHz). For MS, the mass range was 600−3000 m/z, and the scan rate was 1 spectrum/s. For MS/MS, the mass range was 300−3000 m/z, and the scan rate was set to accumulate 1 spectrum/s. The isolation width for MS/MS was set to wide (∼9 amu). For targeted MS/MS, the max time between MS1 spectra was 5 s. ECciD was used for fragmentation.

Electromagnetostatic ExD Cell. The e-MSion ExD cell mounted on a shortened collision cell replaced Agilent's standard CID cell, Figure 1B. The ExD cell consists of a hot

https://doi.org/10.1021/jasms.0c00484
J. Am. Soc. Mass Spectrom. XXXX, XXX, XXX−XXX

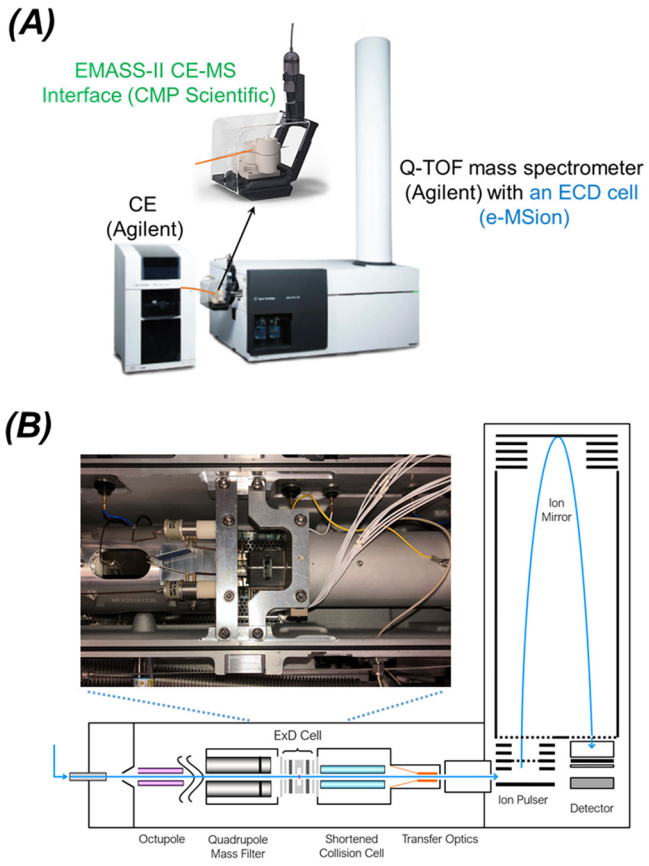

Figure 1. (A) Image of the CZE-MS system including a 7100 Agilent CE system, an EMASS-II CE-MS interface from the CMP Scientific, and an Agilent 6545XT Q-TOF mass spectrometer with an ECD cell. The image was adapted from https://www.agilent.com/cs/library/applications/application-nistmab-charge-variants-cief-ms-5994-1079en-agilent.pdf. (B) Schematic of Agilent 6545XT AdvanceBio Q-TOF mass spectrometer with built-in ExD cell (e-MSion). The inset shows an image of the ExD cell installed between quadrupole and shortened collision cell. The figure was kindly provided by e-MSion.

rhenium filament producing electrons and two high-temperature magnets that restrain electrons radially to the central axis. The analyte ions are guided through the cell without trapping by seven DC electrostatic lens. An auxiliary electronics controller for the ExD cell was interfaced to the instrument computer.[55] The ExD cell was tuned with a direct infusion of substance P, ubiquitin, and CA using our CZE system. The ExD cell was first tuned to achieve full ion transmission without ECD in MS1 and saved as ECD off mode. Then the ExD cell and filament current were optimized to achieve the maximum ECD fragment ion intensity in MS/MS and saved as ECD on mode. During the experiment, the ExD Controller software communicated with the Agilent Mass Hunter software and automatically switched the off and on modes for MS and MS/MS. We empirically set the ECD filament current to 2.6 A to maximize ECD fragmentation. The ECD filament stayed on in both the ECD off and on modes. The optimized ECD conditions, including electrostatic potentials and filament current settings, are shown in Table 1.

Data Analysis. Annotation of standard proteins used MS/MS spectra manually averaged over each electrophoretic peak with Agilent's MassHunter Qualitative Navigator B.08.00. About 20 MS/MS spectra were averaged for each protein. The

Table 1. Optimized ExD Cell Settings for the ECD (ECD on) and Positive Transmission without ECD (ECD off)

settings	ECD on	ECD off
lens 1 (V)	28.0	20.0
lens 2 (V)	−23.5	1.2
lens 3 (V)	33.0	25.8
lens 4 (V)	41.0	27.2
lens 5 (V)	31.5	29.3
lens 6 (V)	26.0	24.7
filament bias (V)	23.0	21.8
filament current (A)	2.6	2.6

information in the averaged MS/MS spectra for each protein including m/z and intensity of ions were exported as an .mgf file. After that, each .mgf file was loaded into the LcMsSpectator (https://omics.pnl.gov/software/lcmsspectator) to match and annotate fragment ions. The sequences of standard proteins were obtained from UniProt (https://www.uniprot.org/). Fragmentation patterns and backbone cleavage coverages were generated by the LcMsSpectator. Matched fragment ion types were b, y, c, z (z and z$^{\bullet}$), and w with a 20 ppm mass tolerance and minimum S/N threshold as 3. The data were also manually checked. The matched fragment ions of proteins exported from the LcMsSpectator are listed in the Supporting Information.

RESULTS AND DISCUSSION

Five types of fragment ions (b, y, c, z, and w ions) were considered for the ECciD in the data analysis using the LcMsSpectator. The z ions in this work represent both z and z$^{\bullet}$ ions. The w ions are from the secondary fragmentation of z$^{\bullet}$ ions through side-chain neutral loss that allows isobaric amino acid residues like leucine (L) and isoleucine (I) to be distinguished in protein sequences.[61] In the human proteome, these two amino acids constitute approximately 16% of the human proteome. Isoleucine and leucine offer distinctive side chain neutral loss, $^{\bullet}C_2H_5$ (29 Da) and $^{\bullet}C_3H_7$ (43 Da), respectively.

We speculated that both the charge state of protein precursor ions and CID potential could influence the overall cleavage coverage of proteins from ECciD in our system. The number of positive charges carried by protein ions affects the positive charge density of proteins, impacting the electron capture during ECD. Too high CID potential would produce evident CID fragmentation of the ECD fragment ions, leading to much more complicated MS/MS spectra and challenges for data interpretation.

Optimization of the Charge State of Protein Ions for ECciD Fragmentation. We optimized the precursor fragmentation from ECciD regarding the protein charge state for the protein mixture using the CZE-Q-TOF system under targeted MS/MS mode. A low CID potential (10 V) was used in the ECciD experiment. The CZE achieved baseline and reproducible separation of the standard proteins with relative standard deviations (RSDs) of migration time less than 2%, Figure S1, which facilitated the method set up for the targeted MS/MS analyses of the protein mixture.

We observed that it was hard to achieve extensive fragmentation of BSA (66 kDa) and CA (29 kDa) under our current ECciD conditions due to their relatively high masses. The backbone cleavage coverage of BSA and CA ranged from 15% to 30%. The CZE-ECciD achieved at least 96% backbone

https://doi.org/10.1021/jasms.0c00484
J. Am. Soc. Mass Spectrom. XXXX, XXX, XXX−XXX

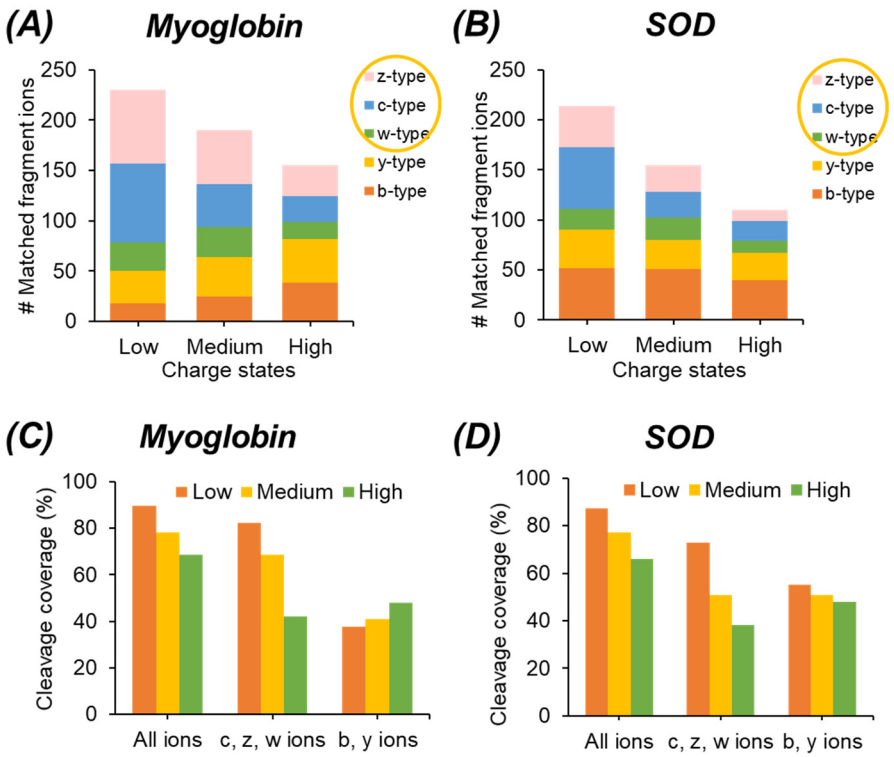

Figure 2. Number of matched fragment ions (A, B) and backbone cleavage coverage (C, D) from ECciD fragmentation of myoglobin and SOD as a function of the precursor's charge state. Myoglobin: low charge: 1060 m/z, +16; medium charge: 893 m/z, +19; high charge: 772 m/z, +22. SOD: low charge: 928 m/z, +17; medium charge: 830 m/z,+19; high charge: 751 m/z, +21. The CID potential was 10 V.

cleavage coverage of ubiquitin from one charge state (+7) due to its small mass (8.6 kDa), Figure S2. Therefore, we focused on myoglobin and SOD in this part. We selected three charge states (low, medium, and high) for each protein to make sure that these charge states were significantly different from each other and had comparable intensity. The medium charge state was the most abundant. We used the CZE-ECciD to separate the standard protein mixture and fragment the specific charge states of the proteins in the targeted MS/MS mode. About 20−60 MS/MS spectra were acquired for each charge state of each protein. The MS/MS spectra were averaged, followed by fragment identification using the LcMsSpectator software.

The protein charge state altered the number of sequence-informative fragment ions (Figure 2A,B) and the backbone cleavage coverage (Figure 2C,D) materially. The total number of fragment ions dropped obviously as the charge state changed from low to high for myoglobin and SOD. When we examined the changes of the number of different types of fragment ions as a function of precursor charge state, we observed that the numbers of c, z, and w ions for the two proteins all declined dramatically at the high charge states compared to the low charge states. The result is different from that in many other studies which generally showed increased ECD/ETD fragmentation efficiency with higher precursor charge states. This could be because ECD filament current was set to the maximum value (2.6 A) in our experiment, causing over fragmentation of precursors at high charge states.

However, the numbers of b and y ions for myoglobin show different trends from the c, z, and w ions. The high charge state of myoglobin produced more b and y ions than its low charge state, providing clear evidence of secondary fragmentation because the higher protein charge state benefited both the electron capture for ECD and protein unfolding for CID. In contrast, SOD generated fewer b and y ions at the high charge state compared to the low charge state. Although myoglobin (17 kDa) has a similar mass to SOD (16 kDa), it was not as well denatured as SOD because SOD was treated with 8 M urea, DTT and IAA before the analysis. Compared to myoglobin ions, the complete unfolding of SOD ions most likely resulted in a higher chance of over fragmentation of their ECD ions during CID.

The backbone cleavage coverage data agree well with the matched fragment ion data. Although the charge state of precursors could influence their backbone cleavage coverage from ECciD significantly, our CZE-ECciD Q-TOF system provided reasonably extensive protein backbone cleavages for the two proteins lower than 20 kDa across a wide range of charge states, which is extremely useful for the dTDP of complex protein mixtures in the widely used data-dependent acquisition (DDA) mode. The system provided 66% (high, +21) to 87% (low, +17) backbone cleavage coverage for SOD, and 68% (high, +22) to 90% (low, +16) backbone cleavage coverage for myoglobin. The optimized charge states of myoglobin and SOD for ECciD in our following experiments were +16 and +17, respectively.

Optimization of the CID Potential for ECciD Fragmentation of Small Proteins. We further optimized the CID potential for ECciD fragmentation of small proteins using the CZE-ECciD system in the targeted MS/MS mode. We focused on myoglobin (+16) and SOD (+17) in the experiment. Six different CID potentials (0, 5, 10, 15, 20, and 30 V) were studied, and triplicate CZE-MS/MS runs were performed for each CID potential.

When a low CID potential (0 or 5 V) was applied for activating/fragmenting the ECD fragment ions, the c and z ions were the dominant types of fragment ions for the two

https://doi.org/10.1021/jasms.0c00484
J. Am. Soc. Mass Spectrom. XXXX, XXX, XXX−XXX

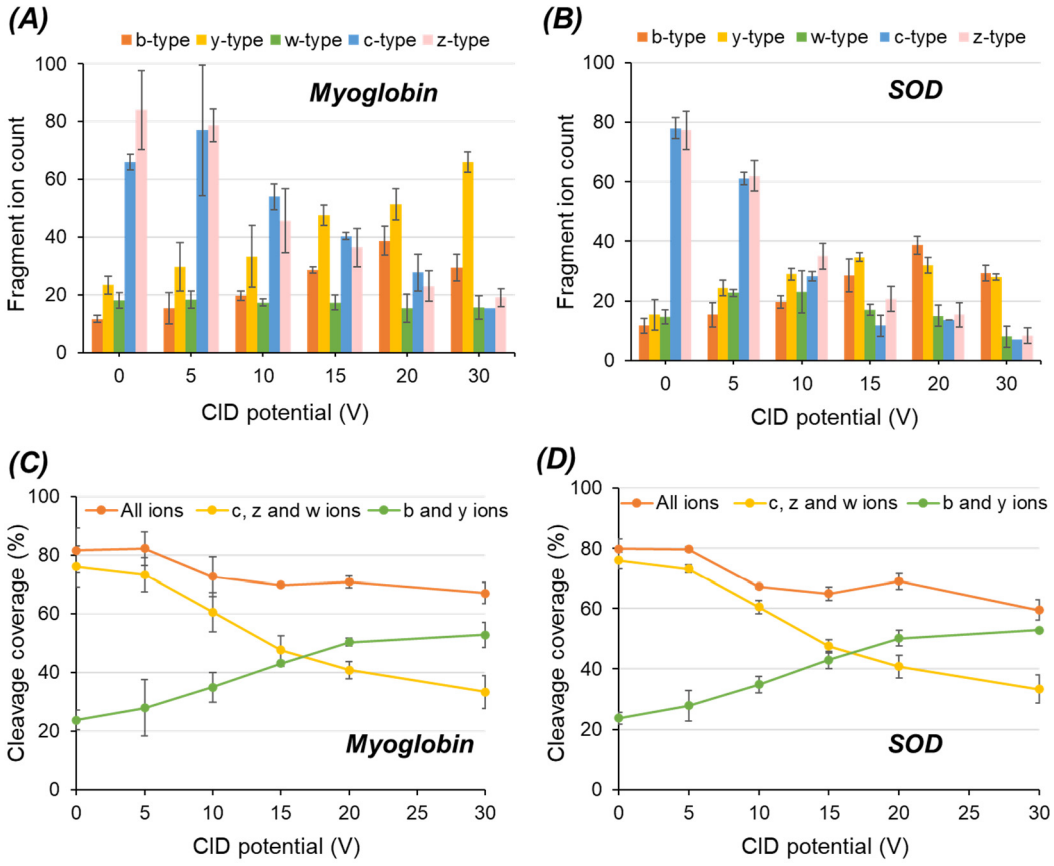

Figure 3. Number of matched fragment ions and backbone cleavage coverage of myoglobin (A and C) and SOD (B and D) from CZE-ECciD as a function of CID potential. The error bars represent the standard deviations of the number of matched fragment ions or the cleavage coverage from triplicate CZE-MS/MS analyses.

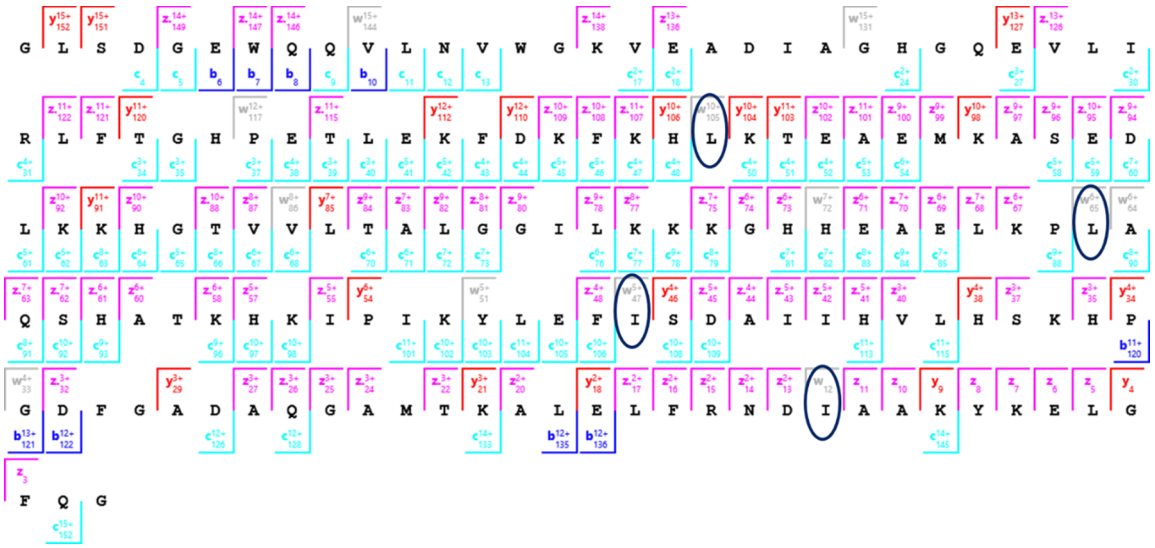

Figure 4. Sequence and fragmentation pattern of myoglobin from CZE-ECciD with a 5-V CID potential. The matched b ions (blue color), y ions (red color), c ions (light blue color), z ions (pink color), and w ions (gray color) were marked on the protein sequence. The four I and L amino acids highlighted with blue circles were determined on the basis of the w ions.

proteins, Figure 3A,B. When the CID potential grew from 10 to 30 V, the b and y ions gradually replaced c and z ions and became the dominant fragment ions. The data demonstrate a clear transition of ECciD from ECD-like to CID-like as the CID energy increased.

The backbone cleavage coverage data (Figure 3C,D) agree reasonably well with the fragment ion data. The 0 and 5 V CID potentials produced comparable overall cleavage coverage from all fragment ions for myoglobin and SOD (~80%), which is significantly higher than that generated by 10−30 V CID potentials. We noted that the overall cleavage coverage of

https://doi.org/10.1021/jasms.0c00484
J. Am. Soc. Mass Spectrom. XXXX, XXX, XXX−XXX

ubiquitin (8.6 kDa, +7) was maintained at about 90% when the CID potential varied from 0 to 30 V. The data suggest that ECciD with a 0−5 V CID potential on the Q-TOF is most likely sufficient enough for extensive fragmentation of proteins lower than 20 kDa.

We note that the backbone cleavage coverage data of ubiquitin, myoglobin and SOD from the charge-state and CID-potential experiments are significantly different even with the same CID potential (10 V) and the same charge states. For example, the ECciD with a 10-V CID potential produced 90% and 73% cleavage coverage of myoglobin (+16) in the two experiments. The phenomenon is because the two experiments were performed several months apart, and it is challenging to maintain the same performance of ECD and Q-TOF in the two experiments.

The w ions from ECciD facilitate the distinguishment of isobaric I and L amino acids in protein sequences. For instance, we identified on average 219 fragment ions (c, z, w, b, and y) of myoglobin using ECciD (5-V CID potential), including 18 ± 3 w ions from triplicate CZE-MS/MS analyses. As shown in Figure 4, the ECciD with a 5-V CID potential produced a comprehensive cleavage coverage of myoglobin, and the w ions distinguished the I and L amino acids at multiple positions in the protein sequence.

Comparison of the CZE-ECciD Data and the Literature Data Regarding Protein Cleavage Coverage. We further compared our CZE-ECciD data with the literature data regarding backbone cleavage coverage of proteins. Our CZE-ECciD system produced 80−90% cleavage coverage of myoglobin. Weisbrod et al. achieved about 70% cleavage coverage of myoglobin by direct-infusion MS using ETD on a 21 T FT-ICR mass spectrometer.[62] Riley et al. observed about 90% and 80% cleavage coverage of myoglobin on an Orbitrap Fusion Lumos mass spectrometer using AI-ETD and a combination of ETD and HCD (EThcD), respectively, through a direct infusion.[63] Brunner et al. obtained nearly 80% cleavage coverage of a 17.5-kDa protein using EThcD on an Orbitrap Fusion mass spectrometer via direct infusion.[64] The data suggest that our CZE-ECciD on a Q-TOF mass spectrometer can achieve comparable cleavage coverage of small proteins (i.e., myoglobin) with direct-infusion MS studies using ETD, AI-ETD, and EThcD on high-end orbitrap mass spectrometers.

The literature direct-infusion studies mentioned above typically employed extensive spectral averaging, while our study only averaged the MS/MS spectra across the 1−2 min protein peaks (myoglobin and SOD), Figure S1. In addition, in our study, less than 200 ng of the protein mixture were consumed for each CZE-ECciD analysis, and only a couple of μL of the sample solution was needed in the sample vial for sample injection for CZE-ECciD. Specifically, only 6 ng and 24 ng of ubiquitin and myoglobin were consumed in each run. The data suggest that the CZE-ECciD platform has high fragmentation sensitivity, which is vital for top-down proteomics analysis of low-abundance proteoforms in complex biological samples.

CONCLUSIONS

We presented a novel analytical tool for dTDP of small proteins (lower than 20 kDa) by combining highly efficient CZE separation and extensive ECciD fragmentation of proteins on an Agilent 6545XT Q-TOF mass spectrometer.

Some improvement in the technique and data analysis software still needs to be done to allow routine and large-scale dTDP using the CZE-ECciD Q-TOF system. First, we need to enable real-time mass calibration during CZE-MS on the Agilent Q-TOF system, which will ensure high mass accuracy of fragment ions, improving the confidence of fragment ion matching. Second, spectral averaging is extremely useful for enhancing the cleavage coverage of proteins from ECD. Incorporating some spectral averaging function in the available dTDP software packages will allow the automated analysis of the ECD data. Third, the widely used dTDP software packages for proteoform identification via database search were developed mainly based on data from Orbitrap and FT-ICR mass spectrometers. Some efforts need to be made to modify the current software tools for analyzing the CZE-ECciD Q-TOF data of complex proteomes. Lastly, we need to improve the ECciD on the Q-TOF system for extensive fragmentation of proteins larger than 30 kDa.

ASSOCIATED CONTENT

Supporting Information

The Supporting Information is available free of charge at https://pubs.acs.org/doi/10.1021/jasms.0c00484.

Matched fragment ions of the standard proteins (XLSX)
Base peak electropherograms of the protein mixture (Figure S1), the annotated MS/MS spectrum and fragmentation pattern of ubiquitin (Figure S2) (PDF)

AUTHOR INFORMATION

Corresponding Author

Liangliang Sun − *Department of Chemistry, Michigan State University, East Lansing, Michigan 48824, United States;* orcid.org/0000-0001-8939-5042; Phone: 517-353-0498; Email: lsun@chemistry.msu.edu

Authors

Xiaojing Shen − *Department of Chemistry, Michigan State University, East Lansing, Michigan 48824, United States;* orcid.org/0000-0003-2079-9115

Tian Xu − *Department of Chemistry, Michigan State University, East Lansing, Michigan 48824, United States*

Blake Hakkila − *e-MSion, Inc., Corvallis, Oregon 97330, United States*

Mike Hare − *e-MSion, Inc., Corvallis, Oregon 97330, United States*

Qianjie Wang − *Department of Chemistry, Michigan State University, East Lansing, Michigan 48824, United States*

Qianyi Wang − *Department of Chemistry, Michigan State University, East Lansing, Michigan 48824, United States*

Joseph S. Beckman − *e-MSion, Inc., Corvallis, Oregon 97330, United States; Linus Pauling Institute and the Department of Biochemistry and Biophysics, Oregon State University, Corvallis, Oregon 97331, United States*

Complete contact information is available at: https://pubs.acs.org/10.1021/jasms.0c00484

Author Contributions

#Xiaojing Shen and Tian Xu contribute equally to this work.

Notes

The authors declare the following competing financial interest(s): The authors are collaborating with Agilent, e-MSion and CMP Scientific.

■ ACKNOWLEDGMENTS

We thank Agilent, e-MSion, and CMP Scientific for their kind support for this project. In particular, we thank John Sausen (Director of Strategic Initiatives-Mass Spectrometry), Dr. David Wong, and Dr. Rebecca Glaskin at Agilent for their useful suggestions about the ECciD data. We acknowledge support from the National Science Foundation (CAREER Award, Grant No. DBI1846913) and the National Institutes of Health (Grant No. R01GM125991).

■ REFERENCES

(1) Smith, L. M.; Kelleher, N. L. Proteoforms as the Next Proteomics Currency. *Science* **2018**, *359* (6380), 1106−1107.
(2) Yang, X.; Coulombe-Huntington, J.; Kang, S.; Sheynkman, G. M.; Hao, T.; Richardson, A.; Sun, S.; Yang, F.; Shen, Y. A.; Murray, R. R.; Spirohn, K.; Begg, B. E.; Duran-Frigola, M.; MacWilliams, A.; Pevzner, S. J.; Zhong, Q.; Trigg, S. A.; Tam, S.; Ghamsari, L.; Sahni, N.; Yi, S.; Rodriguez, M. D.; Balcha, D.; Tan, G.; Costanzo, M.; Andrews, B.; Boone, C.; Zhou, X. J.; Salehi-Ashtiani, K.; Charloteaux, B.; Chen, A. A.; Calderwood, M. A.; Aloy, P.; Roth, F. P.; Hill, D. E.; Iakoucheva, L. M.; Xia, Y.; Vidal, M. Widespread Expansion of Protein Interaction Capabilities by Alternative Splicing. *Cell* **2016**, *164* (4), 805−817.
(3) Li, Y. I.; van de Geijn, B.; Raj, A.; Knowles, D. A.; Petti, A. A.; Golan, D.; Gilad, Y.; Pritchard, J. K. RNA Splicing is A Primary Link between Genetic Variation and Disease. *Science* **2016**, *352* (6285), 600−604.
(4) Costa, H. A.; Leitner, M. G.; Sos, M. L.; Mavrantoni, A.; Rychkova, A.; Johnson, J. R.; Newton, B. W.; Yee, M. C.; De La Vega, F. M.; Ford, J. M.; Krogan, N. J.; Shokat, K. M.; Oliver, D.; Halaszovich, C. R.; Bustamante, C. D. Discovery and Functional Characterization of A Neomorphic PTEN Mutation. *Proc. Natl. Acad. Sci. U. S. A.* **2015**, *112* (45), 13976−13981.
(5) Ntai, I.; Fornelli, L.; DeHart, C. J.; Hutton, J. E.; Doubleday, P. F.; LeDuc, R. D.; van Nispen, A. J.; Fellers, R. T.; Whiteley, G.; Boja, E. S.; Rodriguez, H.; Kelleher, N. L. Precise Characterization of Kras4b Proteoforms in Human Colorectal Cells and Tumors Reveals Mutation/Modification Cross-Talk. *Proc. Natl. Acad. Sci. U. S. A.* **2018**, *115* (16), 4140−4145.
(6) Jenuwein, T. Translating the Histone Code. *Science* **2001**, *293* (5532), 1074−1080.
(7) Toby, T. K.; Fornelli, L.; Kelleher, N. L. Progress In Top-Down Proteomics And The Analysis Of Proteoforms. *Annu. Rev. Anal. Chem.* **2016**, *9* (1), 499−519.
(8) Chen, B.; Brown, K. A.; Lin, Z.; Ge, Y. Top-Down Proteomics: Ready for Prime Time? *Anal. Chem.* **2018**, *90* (1), 110−127.
(9) Cai, W.; Tucholski, T.; Chen, B.; Alpert, A. J.; McIlwain, S.; Kohmoto, T.; Jin, S.; Ge, Y. Top-Down Proteomics of Large Proteins up to 223 kDa Enabled by Serial Size Exclusion Chromatography Strategy. *Anal. Chem.* **2017**, *89* (10), 5467−5475.
(10) Ansong, C.; Wu, S.; Meng, D.; Liu, X.; Brewer, H. M.; Deatherage Kaiser, B. L.; Nakayasu, E. S.; Cort, J. R.; Pevzner, P.; Smith, R. D.; Heffron, F.; Adkins, J. N.; Pasa-Tolic, L. Top-down Proteomics Reveals A Unique Protein S-thiolation Switch in Salmonella Typhimurium In Response To Infection-like Conditions. *Proc. Natl. Acad. Sci. U. S. A.* **2013**, *110* (25), 10153−10158.
(11) Tran, J. C.; Zamdborg, L.; Ahlf, D. R.; Lee, J. E.; Catherman, A. D.; Durbin, K. R.; Tipton, J. D.; Vellaichamy, A.; Kellie, J. F.; Li, M.; Wu, C.; Sweet, S. M.; Early, B. P.; Siuti, N.; LeDuc, R. D.; Compton, P. D.; Thomas, P. M.; Kelleher, N. L. Mapping Intact Protein Isoforms in Discovery Mode Using Top-down Proteomics. *Nature* **2011**, *480* (7376), 254−258.
(12) Shen, Y.; Tolić, N.; Piehowski, P. D.; Shukla, A. K.; Kim, S.; Zhao, R.; Qu, Y.; Robinson, E.; Smith, R. D.; Paša-Tolić, L. High-Resolution Ultrahigh-Pressure Long Column Reversed-Phase Liquid Chromatography for Top-Down Proteomics. *J. Chromatogr. A* **2017**, *1498*, 99−110.
(13) Catherman, A. D.; Durbin, K. R.; Ahlf, D. R.; Early, B. P.; Fellers, R. T.; Tran, J. C.; Thomas, P. M.; Kelleher, N. L. Large-Scale Top-Down Proteomics of the Human Proteome: Membrane Proteins, Mitochondria, and Senescence. *Mol. Cell. Proteomics* **2013**, *12* (12), 3465−3473.
(14) Anderson, L. C.; DeHart, C. J.; Kaiser, N. K.; Fellers, R. T.; Smith, D. F.; Greer, J. B.; LeDuc, R. D.; Blakney, G. T.; Thomas, P. M.; Kelleher, N. L.; Hendrickson, C. L. Identification and Characterization of Human Proteoforms by Top-Down LC-21 T FT-ICR Mass Spectrometry. *J. Proteome Res.* **2017**, *16* (2), 1087−1096.
(15) Schaffer, L. V.; Rensvold, J. W.; Shortreed, M. R.; Cesnik, A. J.; Jochem, A.; Scalf, M.; Frey, B. L.; Pagliarini, D. J.; Smith, L. M. Identification and Quantification of Murine Mitochondrial Proteoforms Using an Integrated Top-Down and Intact-Mass Strategy. *J. Proteome Res.* **2018**, *17* (10), 3526−3536.
(16) Yu, D.; Wang, Z.; Cupp-Sutton, K. A.; Liu, X.; Wu, S. Deep Intact Proteoform Characterization in Human Cell Lysate Using High-pH and Low-pH Reversed-Phase Liquid Chromatography. *J. Am. Soc. Mass Spectrom.* **2019**, *30* (12), 2502−2513.
(17) Fornelli, L.; Durbin, K. R.; Fellers, R. T.; Early, B. P.; Greer, J. B.; LeDuc, R. D.; Compton, P. D.; Kelleher, N. L. Advancing Top-down Analysis of the Human Proteome Using A Benchtop Quadrupole-Orbitrap Mass Spectrometer. *J. Proteome Res.* **2017**, *16* (2), 609−618.
(18) Aebersold, R.; Agar, J. N.; Amster, I. J.; Baker, M. S.; Bertozzi, C. R.; Boja, E. S.; Costello, C. E.; Cravatt, B. F.; Fenselau, C.; Garcia, B. A.; Ge, Y.; Gunawardena, J.; Hendrickson, R. C.; Hergenrother, P. J.; Huber, C. G.; Ivanov, A. R.; Jensen, O. N.; Jewett, M. C.; Kelleher, N. L.; Kiessling, L. L.; Krogan, N. J.; Larsen, M. R.; Loo, J. A.; Ogorzalek Loo, R. R.; Lundberg, E.; MacCoss, M. J.; Mallick, P.; Mootha, V. K.; Mrksich, M.; Muir, T. W.; Patrie, S. M.; Pesavento, J. J.; Pitteri, S. J.; Rodriguez, H.; Saghatelian, A.; Sandoval, W.; Schluter, H.; Sechi, S.; Slavoff, S. A.; Smith, L. M.; Snyder, M. P.; Thomas, P. M.; Uhlen, M.; Van Eyk, J. E.; Vidal, M.; Walt, D. R.; White, F. M.; Williams, E. R.; Wohlschlager, T.; Wysocki, V. H.; Yates, N. A.; Young, N. L.; Zhang, B. How Many Human Proteoforms Are There? *Nat. Chem. Biol.* **2018**, *14* (3), 206−214.
(19) Lubeckyj, R. A.; McCool, E. N.; Shen, X.; Kou, Q.; Liu, X.; Sun, L. Single-Shot Top-down Proteomics with Capillary Zone Electrophoresis-Electrospray Ionization-Tandem Mass Spectrometry for Identification of Nearly 600 Escherichia coli Proteoforms. *Anal. Chem.* **2017**, *89* (22), 12059−12067.
(20) McCool, E. N.; Lubeckyj, R. A.; Shen, X.; Chen, D.; Kou, Q.; Liu, X.; Sun, L. Deep Top-Down Proteomics Using Capillary Zone Electrophoresis-Tandem Mass Spectrometry: Identification of 5700 Proteoforms from the Escherichia coli Proteome. *Anal. Chem.* **2018**, *90* (9), 5529−5533.
(21) Lubeckyj, R. A.; Basharat, A. R.; Shen, X.; Liu, X.; Sun, L. Large-Scale Qualitative and Quantitative Top-Down Proteomics Using Capillary Zone Electrophoresis-Electrospray Ionization-Tandem Mass Spectrometry with Nanograms of Proteome Samples. *J. Am. Soc. Mass Spectrom.* **2019**, *30* (8), 1435−1445.
(22) Shen, X.; Yang, Z.; McCool, E. N.; Lubeckyj, R. A.; Chen, D.; Sun, L. Capillary Zone Electrophoresis-Mass Spectrometry for Top-down Proteomics. *TrAC, Trends Anal. Chem.* **2019**, *120*, 115644.
(23) Han, X.; Wang, Y.; Aslanian, A.; Bern, M.; Lavallée-Adam, M.; Yates, J. R., 3rd. Sheathless Capillary Electrophoresis-Tandem Mass Spectrometry for Top-down Characterization of Pyrococcus Furiosus Proteins on A Proteome Scale. *Anal. Chem.* **2014**, *86* (22), 11006−11012.
(24) Haselberg, R.; De Jong, G. J.; Somsen, G. W. Low-Flow Sheathless Capillary Electrophoresis-Mass Spectrometry for Sensitive Glycoform Profiling of Intact Pharmaceutical Proteins. *Anal. Chem.* **2013**, *85* (4), 2289−2296.
(25) Li, Y.; Compton, P. D.; Tran, J. C.; Ntai, I.; Kelleher, N. L. Optimizing Capillary Electrophoresis for Top-down Proteomics of 30−80 KDa Proteins. *Proteomics* **2014**, *14* (10), 1158−1164.

https://doi.org/10.1021/jasms.0c00484
J. Am. Soc. Mass Spectrom. XXXX, XXX, XXX−XXX

(26) Bush, D. R.; Zang, L.; Belov, A. M.; Ivanov, A. R.; Karger, B. L. High Resolution CZE-MS Quantitative Characterization of Intact Biopharmaceutical Proteins: Proteoforms of Interferon-beta1. *Anal. Chem.* **2016**, *88* (2), 1138−1146.
(27) Zhao, Y.; Sun, L.; Champion, M. M.; Knierman, M. D.; Dovichi, N. J. Capillary Zone Electrophoresis-Electrospray Ionization-Tandem Mass Spectrometry for Top-down Characterization of the Mycobacterium Marinum Secretome. *Anal. Chem.* **2014**, *86* (10), 4873−4878.
(28) Valaskovic, G. A.; Kelleher, N. L.; McLafferty, F. W. Attomole Protein Characterization by Capillary Electrophoresis-Mass Spectrometry. *Science* **1996**, *273* (5279), 1199−1202.
(29) Han, X.; Wang, Y.; Aslanian, A.; Fonslow, B.; Graczyk, B.; Davis, T. N.; Yates, J. R., 3rd. In-line Separation by Capillary Electrophoresis Prior to Analysis by Top-down Mass Spectrometry Enables Sensitive Characterization of Protein Complexes. *J. Proteome Res.* **2014**, *13* (12), 6078−6086.
(30) Krokhin, O. V.; Anderson, G.; Spicer, V.; Sun, L.; Dovichi, N. J. Predicting Electrophoretic Mobility of Tryptic Peptides for High-Throughput CZE-MS Analysis. *Anal. Chem.* **2017**, *89* (3), 2000−2008.
(31) Chen, D.; Ludwig, K. R.; Krokhin, O. V.; Spicer, V.; Yang, Z.; Shen, X.; Hummon, A. B.; Sun, L. Capillary Zone Electrophoresis-Tandem Mass Spectrometry for Large-Scale Phosphoproteomics with the Production of over 11,000 Phosphopeptides from the Colon Carcinoma HCT116 Cell Line. *Anal. Chem.* **2019**, *91* (3), 2201−2208.
(32) Chen, D.; Lubeckyj, R. A.; Yang, Z.; McCool, E. N.; Shen, X.; Wang, Q.; Xu, T.; Sun, L. Predicting Electrophoretic Mobility of Proteoforms for Large-Scale Top-Down Proteomics. *Anal. Chem.* **2020**, *92* (5), 3503−3507.
(33) Maxwell, E. J.; Zhong, X.; Zhang, H.; van Zeijl, N.; Chen, D. D. Decoupling CE and ESI for a more robust interface with MS. *Electrophoresis* **2010**, *31* (7), 1130−1137.
(34) Wojcik, R.; Dada, O. O.; Sadilek, M.; Dovichi, N. Simplified capillary electrophoresis nanospray sheath-flow interface for high efficiency and sensitive peptide analysis. *Rapid Commun. Mass Spectrom.* **2010**, *24* (17), 2554−2560.
(35) Sun, L.; Zhu, G.; Zhang, Z.; Mou, S.; Dovichi, N. J. Third-Generation Electrokinetically Pumped Sheath-Flow Nanospray Interface with Improved Stability and Sensitivity for Automated Capillary Zone Electrophoresis−Mass Spectrometry Analysis of Complex Proteome Digests. *J. Proteome Res.* **2015**, *14* (5), 2312−2321.
(36) Choi, S. B.; Zamarbide, M.; Manzini, M. C.; Nemes, P. Tapered-Tip Capillary Electrophoresis Nano-Electrospray Ionization Mass Spectrometry for Ultrasensitive Proteomics: the Mouse Cortex. *J. Am. Soc. Mass Spectrom.* **2017**, *28* (4), 597−607.
(37) Moini, M. Simplifying CE-MS Operation. 2. Interfacing Low-Flow Separation Techniques to Mass Spectrometry Using A Porous Tip. *Anal. Chem.* **2007**, *79* (11), 4241−4246.
(38) Syka, J. E. P.; Coon, J. J.; Schroeder, M. J.; Shabanowitz, J.; Hunt, D. F. Peptide and protein sequence analysis by electron transfer dissociation mass spectrometry. *Proc. Natl. Acad. Sci. U. S. A.* **2004**, *101* (26), 9528−9533.
(39) Riley, N. M.; Sikora, J. W.; Seckler, H. S.; Greer, J. B.; Fellers, R. T.; LeDuc, R. D.; Westphall, M. S.; Thomas, P. M.; Kelleher, N. L.; Coon, J. J. The Value of Activated Ion Electron Transfer Dissociation for High-Throughput Top-Down Characterization of Intact Proteins. *Anal. Chem.* **2018**, *90* (14), 8553−8560.
(40) McCool, E. N.; Lodge, J. M.; Basharat, A. R.; Liu, X.; Coon, J. J.; Sun, L. Capillary Zone Electrophoresis-Tandem Mass Spectrometry with Activated Ion Electron Transfer Dissociation for Large-scale Top-down Proteomics. *J. Am. Soc. Mass Spectrom.* **2019**, *30* (12), 2470−2479.
(41) Li, H.; Nguyen, H. H.; Ogorzalek-Loo, R. R.; Campuzano, I. D. G.; Loo, J. A. An Integrated Native Mass Spectrometry and Top-down Proteomics Method that Connects Sequence to Structure and Function of Macromolecular Complexes. *Nat. Chem.* **2018**, *10* (2), 139−148.
(42) Voinov, V. G.; Deinzer, M. L.; Barofsky, D. F. Electron Capture Dissociation in a Linear Radiofrequency-Free Magnetic Cell. *Rapid Commun. Mass Spectrom.* **2008**, *22* (19), 3087−3088.
(43) Voinov, V. G.; Deinzer, M. L.; Beckman, J. S.; Barofsky, D. F. Electron Capture, Collision-Induced, and Electron Capture-Collision Induced Dissociation in Q-TOF. *J. Am. Soc. Mass Spectrom.* **2011**, *22* (4), 607−611.
(44) Shaw, J. B.; Malhan, N.; Vasil'ev, Y. V.; Lopez, N. I.; Makarov, A. A.; Beckman, J. S.; Voinov, V. G. Sequencing Grade Tandem Mass Spectrometry for Top−Down Proteomics Using Hybrid Electron Capture Dissociation Methods in a Benchtop Orbitrap Mass Spectrometer. *Anal. Chem.* **2018**, *90* (18), 10819−10827.
(45) Tucholski, T.; Knott, S. J.; Chen, B.; Pistono, P.; Lin, Z.; Ge, Y. A Top-Down Proteomics Platform Coupling Serial Size Exclusion Chromatography and Fourier Transform Ion Cyclotron Resonance Mass Spectrometry. *Anal. Chem.* **2019**, *91* (6), 3835−3844.
(46) Shaw, J. B.; Li, W.; Holden, D. D.; Zhang, Y.; Griep-Raming, J.; Fellers, R. T.; Early, B. P.; Thomas, P. M.; Kelleher, N. L.; Brodbelt, J. S. Complete Protein Characterization Using Top-Down Mass Spectrometry and Ultraviolet Photodissociation. *J. Am. Chem. Soc.* **2013**, *135* (34), 12646−12651.
(47) Greer, S. M.; Brodbelt, J. S. Top-Down Characterization of Heavily Modified Histones Using 193 nm Ultraviolet Photodissociation Mass Spectrometry. *J. Proteome Res.* **2018**, *17* (3), 1138−1145.
(48) Fornelli, L.; Srzentić, K.; Toby, T. K.; Doubleday, P. F.; Huguet, R.; Mullen, C.; Melani, R. D.; dos Santos Seckler, H.; DeHart, C. J.; Weisbrod, C. R.; Durbin, K. R.; Greer, J. B.; Early, B. P.; Fellers, R. T.; Zabrouskov, V.; Thomas, P. M.; Compton, P. D.; Kelleher, N. L. Thorough Performance Evaluation of 213 Nm Ultraviolet Photodissociation for Top-Down Proteomics. *Mol. Cell. Proteomics* **2020**, *19* (2), 405−420.
(49) McCool, E. N.; Chen, D.; Li, W.; Liu, Y.; Sun, L. Capillary Zone Electrophoresis-Tandem Mass Spectrometry with Ultraviolet Photodissociation (213 nm) for Large-scale Top−down Proteomics. *Anal. Methods* **2019**, *11* (22), 2855−2861.
(50) Zubarev, R. A.; Kelleher, N. L.; McLafferty, F. W. Electron Capture Dissociation of Multiply Charged Protein Cations. A Nonergodic Process. *J. Am. Chem. Soc.* **1998**, *120* (13), 3265−3266.
(51) Zubarev, R. A.; Kruger, N. A.; Fridriksson, E. K.; Lewis, M. A.; Horn, D. M.; Carpenter, B. K.; McLafferty, F. W. Electron Capture Dissociation of Gaseous Multiply-Charged Proteins Is Favored at Disulfide Bonds and Other Sites of High Hydrogen Atom Affinity. *J. Am. Chem. Soc.* **1999**, *121* (12), 2857−2862.
(52) Horn, D. M.; Ge, Y.; McLafferty, F. W. Activated Ion Electron Capture Dissociation for Mass Spectral Sequencing of Larger (42 kDa) Proteins. *Anal. Chem.* **2000**, *72* (20), 4778−4784.
(53) Ge, Y.; Lawhorn, B. G.; ElNaggar, M.; Strauss, E.; Park, J.-H.; Begley, T. P.; McLafferty, F. W. Top Down Characterization of Larger Proteins (45 kDa) by Electron Capture Dissociation Mass Spectrometry. *J. Am. Chem. Soc.* **2002**, *124* (4), 672−678.
(54) Zabrouskov, V.; Whitelegge, J. P. Increased Coverage in the Transmembrane Domain with Activated-Ion Electron Capture Dissociation for Top-Down Fourier-Transform Mass Spectrometry of Integral Membrane Proteins. *J. Proteome Res.* **2007**, *6* (6), 2205−2210.
(55) Williams, J. P.; Morrison, L. J.; Brown, J. M.; Beckman, J. S.; Voinov, V. G.; Lermyte, F. Top-Down Characterization of Denatured Proteins and Native Protein Complexes Using Electron Capture Dissociation Implemented within A Modified Ion Mobility-Mass Spectrometer. *Anal. Chem.* **2020**, *92* (5), 3674−3681.
(56) Fort, K. L.; Cramer, C. N.; Voinov, V. G.; Vasil'ev, Y. V.; Lopez, N. I.; Beckman, J. S.; Heck, A. J. R. Exploring ECD on a Benchtop Q Exactive Orbitrap Mass Spectrometer. *J. Proteome Res.* **2018**, *17* (2), 926−933.
(57) Zhou, M.; Liu, W.; Shaw, J. B. Charge Movement and Structural Changes in the Gas-Phase Unfolding of Multimeric Protein Complexes Captured by Native Top-Down Mass Spectrometry. *Anal. Chem.* **2020**, *92* (2), 1788−1795.

https://doi.org/10.1021/jasms.0c00484
J. Am. Soc. Mass Spectrom. XXXX, XXX, XXX−XXX

(58) Zhu, G.; Sun, L.; Dovichi, N. J. Thermally-Initiated Free Radical Polymerization for Reproducible Production of Stable Linear Polyacrylamide Coated Capillaries, and Their Application to Proteomic Analysis Using Capillary Zone Electrophoresis−Mass Spectrometry. *Talanta* **2016**, *146*, 839−843.
(59) McCool, E. N.; Lubeckyj, R.; Shen, X.; Kou, Q.; Liu, X.; Sun, L. Large-scale Top-down Proteomics Using Capillary Zone Electrophoresis Tandem Mass Spectrometry. *J. Vis. Exp.* **2018**, *140*, No. e58644.
(60) Sun, L.; Zhu, G.; Zhao, Y.; Yan, X.; Mou, S.; Dovichi, N. J. Ultrasensitive and Fast Bottom-up Analysis of Femtogram Amounts of Complex Proteome Digests. *Angew. Chem., Int. Ed.* **2013**, *52* (51), 13661−13664.
(61) Kjeldsen, F.; Haselmann, K. F.; Budnik, B. A.; Jensen, F.; Zubarev, R. A. Dissociative capture of hot (3−13 eV) electrons by polypeptide polycations: an efficient process accompanied by secondary fragmentation. *Chem. Phys. Lett.* **2002**, *356* (3), 201−206.
(62) Weisbrod, C. R.; Kaiser, N. K.; Syka, J. E. P.; Early, L.; Mullen, C.; Dunyach, J. J.; English, A. M.; Anderson, L. C.; Blakney, G. T.; Shabanowitz, J.; Hendrickson, C. L.; Marshall, A. G.; Hunt, D. F. Front-End Electron Transfer Dissociation Coupled to a 21 T FT-ICR Mass Spectrometer for Intact Protein Sequence Analysis. *J. Am. Soc. Mass Spectrom.* **2017**, *28* (9), 1787−1795.
(63) Riley, N. M.; Westphall, M. S.; Coon, J. J. Activated Ion-Electron Transfer Dissociation Enables Comprehensive Top-Down Protein Fragmentation. *J. Proteome Res.* **2017**, *16* (7), 2653−2659.
(64) Brunner, A. M.; Lössl, P.; Liu, F.; Huguet, R.; Mullen, C.; Yamashita, M.; Zabrouskov, V.; Makarov, A.; Altelaar, A. F. M.; Heck, A. J. R. Benchmarking multiple fragmentation methods on an orbitrap fusion for top-down phospho-proteoform characterization. *Anal. Chem.* **2015**, *87* (8), 4152−8.

https://doi.org/10.1021/jasms.0c00484
J. Am. Soc. Mass Spectrom. XXXX, XXX, XXX−XXX